



Cite this: *Org. Biomol. Chem.*, 2018, **16**, 7801

Received 5th October 2018,
Accepted 8th October 2018

DOI: 10.1039/c8ob02482k

rsc.li/obc

Triazole-imidazole (TA-IM) derivatives as ultrafast fluorescent probes for selective Ag^+ detection†

Qi Lai,^a Qing Liu,^a Ying He,^b Kai Zhao,^a Chiyu Wei,^b Lukasz Wojtas,^b Xiaodong Shi  ^{*a,b} and Zhiguang Song^{*a}

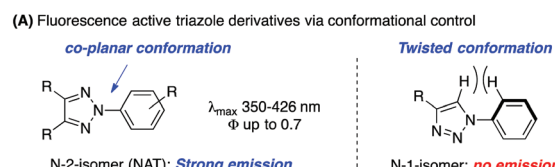
1,2,3-Triazole-imidazole derivatives (TA-IM) were prepared as fluorescent probes for silver ion detection. The design principle is the incorporation of an intramolecular H-bond between the imidazole and triazole moiety that enables a co-planar conformation to achieve fluorescence emission in the UV-blue range. Screening of different metal ions revealed excellent binding affinity of this new class of compounds toward silver ions in aqueous solution. The novel probe provided ultrafast detection (<30 s) even for a very low concentration of silver ions (in the nM range) with good linear correlation, making it a practical sensor for detection of silver ions.

Fluorescence active molecules are of great importance in chemical,¹ biological² and medicinal research.³ A new class of small organic molecules with good fluorescence emission could offer opportunities for interesting applications.⁴ Over the past decade, our group has been working on the development of functional 1,2,3-triazole (TA) compounds as ligands for metal coordination.⁵ A series of triazole ligands have been identified to promote metal-catalyzed reactions.⁶ Upon synthesis of triazole derivatives,⁷ we found that *N*-2 aryl triazole (NAT) showed strong emission in the UV-blue range (λ_{max} between 380 nm and 430 nm). In contrast, the *N*-1 isomer exhibited almost no emission ($\Phi < 0.02$). According to our structural analysis, strong fluorescence emission can be attributed to the co-planar conformation between the triazole ring and *N*-2 aryl groups (Scheme 1A).⁸

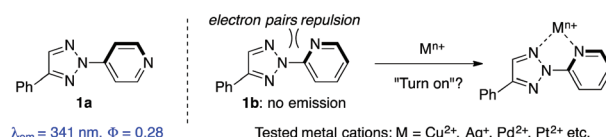
Based on these unique features,⁹ we wondered whether 1,2,3-triazole can be developed as a novel fluorescent probe for metal cation detection upon coordination. Herein, we report imidazole substituted 1,2,3-triazole (TA-IM) derivatives as a

new class of fluorescent active compounds with excellent selectivity toward Ag^+ (over 20 other tested cations) in aqueous media. These new fluorescent probes also gave high sensitivity with a linear concentration–emission correlation. Moreover, compared with other reported Ag^+ detection methods, TA-IM demonstrated an ultrafast response time of less than 30 seconds upon coordination. All these features make TA-IM a new practical sensor for Ag^+ detection.

Our interest in developing triazole derivatives as metal cation sensors originated from the conformational analysis of the *N*-2-aryl triazole (NAT) fluorophore. As shown in Scheme 1B, we have previously demonstrated that 4-pyridyl triazole **1a** showed good fluorescence emission ($\Phi = 0.28$), while the 2-pyridyl isomer **1b** was fluorescence-inactive (no emission). The X-ray crystal structure of **1b** revealed a twisted conformation between the two aromatic rings, likely due to repulsion between the lone pair electrons of nitrogen.⁸ Based on this analysis, we postulated that metal coordination between the two nitrogen atoms in **1b** could force the two aromatic rings to adopt a co-planar conformation and, therefore, may “turn on” the fluorescence emission upon coordination. To confirm this idea, we performed the coordination experiments of **1b** (TA-Py) with various metal cations (Cu^{2+} , Ag^+ , Pd^{2+} , Pt^{2+} ,



(B) Initial design: planar conformation upon coordination

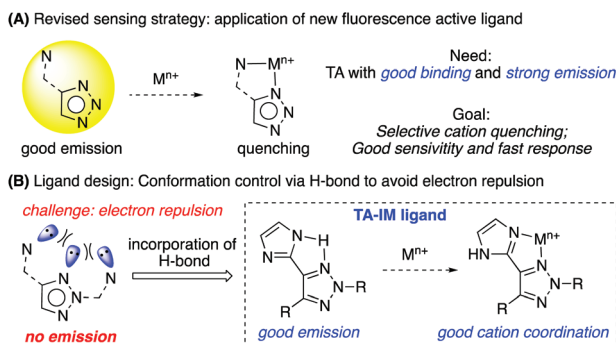


^aState Key Laboratory of Supramolecular Structure and Materials, College of Chemistry, Jilin University, Changchun, Jilin 13002, China. E-mail: szg@jlu.edu.cn

^bThe Department of Chemistry, University of South Florida, 4202 E. Fowler Avenue, Tampa, Florida 33620, United States. E-mail: xmshi@usf.edu

†Electronic supplementary information (ESI) available: Experimental procedures, characterization data, NMR spectra and X-ray data. CCDC 1835133(5a), 1835134(5b), 1835139(5d), 1835140(5i) and 1835141(5k). For ESI and crystallographic data in CIF or other electronic format see DOI: 10.1039/c8ob02482k

Scheme 1 Design of triazole-based fluorescent probes.



Scheme 2 Revised sensing strategy with the TA-IM ligand.

Ni^{2+} etc.). Unfortunately, no fluorescence emission change was observed in all cases (see details in ESI, Fig. S1†). In spite of the possible co-planar conformation upon chelation, the results suggested that NAT's excited state was nevertheless quenched due to potential electron and/or energy transfer upon cation binding.¹⁰ As a result, the initial turn-on sensor hypothesis did not work, and we turned to design a turn-off sensor with a similar framework.

With the assumption that fluorescence quenching occurs upon metal coordination for TA-Py ligand **1b**, we sought out to develop new triazole ligands with both good fluorescence emission and metal binding ability to achieve metal sensing (Scheme 2A).¹¹ As discussed above, no fluorescence emission was observed for the TA-Py ligand due to the nitrogen lone pair electron repulsion (Scheme 2B). To address this problem while keeping the bi-dentate binding nature, we proposed a new ligand system as triazole-imidazole (TA-IM). The key of our design is the incorporation of an intramolecular H-bond to avoid lone pair electron repulsion so as to enhance the formation of a co-planar conformation for effective fluorescence emission while maintaining the bi-dentate nitrogen binding mode. As shown in Fig. 1A, a group of TA-IM compounds was successfully prepared. The structures of these TA-IM compounds are summarized in Fig. 1B.

The X-ray crystal structures of TA-IM were successfully obtained with several TA-IM compounds (**5a**, **5b**, **5d**, **5i** and **5k**), which verified the proposed N-2 isomer conformation. Moreover, as highlighted in Fig. 1B, compared with the C-5 phenyl ring, the C-4 imidazole ring had a much smaller dihedral angle (18.2°) with the triazole ring, which suggested the formation of an intramolecular H-bond. With the TA-IM successfully prepared and the *N*-2-isomer identified, we evaluated their fluorescence emission to verify our initial design that an intramolecular H-bond plays a crucial role in providing conformational control for effective fluorescence emission. The emission spectra of several representative TA-derivatives including TA-IM are shown in Fig. 2.

As expected, TA-IM **5a** and **5g** displayed strong fluorescence emission with quantum yields (Φ_{PL}) of 0.77 and 0.98 respectively. The stronger emission obtained with **5g** over **5a** is likely due to the reduced steric hindrance of C-5-H in **5g** over C-5-Ph

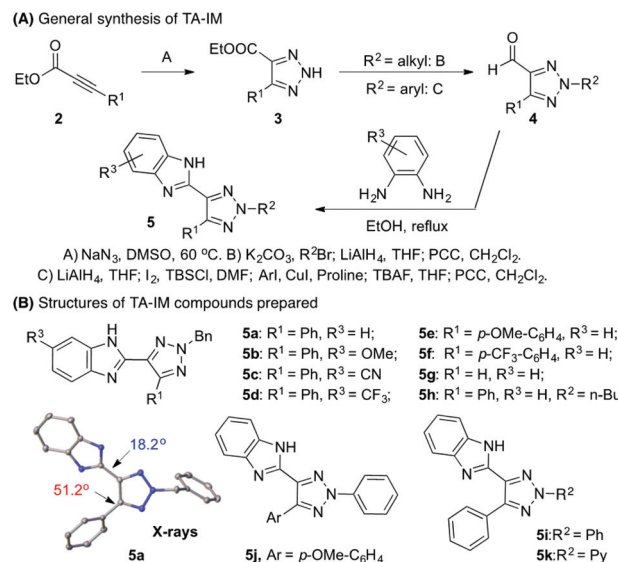
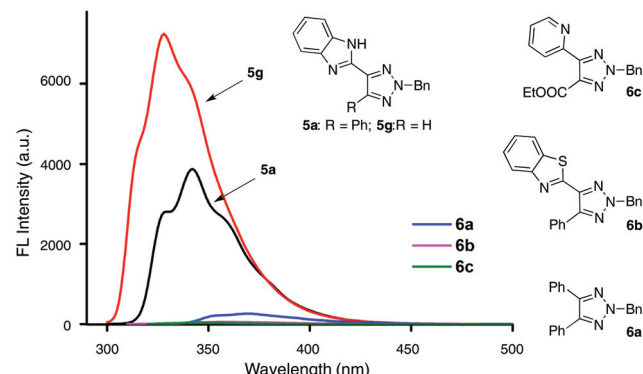


Fig. 1 General synthetic route for TA-IM ligands.

Fig. 2 Fluorescence emission of some TA-IM ligands. Fluorescence emission of compounds **5a**–**6c**. Concentration: $20 \mu\text{mol L}^{-1}$ in EtOH .

in **5a**. This suggested that **5g** favored the co-planar conformation. Switching imidazole to phenyl (**6a**), thiazole (**6b**) and pyridine (**6c**) shut down the fluorescence emission almost completely, which highlights the crucial role of the intramolecular H-bond in achieving the fluorescence-active TA-ligand. Importantly, the fluorescence intensity of **5a** in solution remained the same even after ten months (Fig. S6†), suggesting the excellent stability of the new TA-IM fluorophore. The detailed excitation and emission information of all TA-IM substrates 5 is summarized in Table 1.

As shown in Table 1, all tested TA-IM **5** exhibited strong UV-blue fluorescence emission with λ_{max} between 330 nm and 380 nm. The electron donating group on imidazole (**5b**) caused an emission red-shift while the electron withdrawing group resulted in a slight blue-shift (**5d**). No significant electronic effect was observed on the phenyl substitution (**5e** vs. **5f**). A large red-shift was obtained with conjugated N-2 aryl substrates (**5i**, **5j** and **5k**), similar to the previously reported

Table 1 Optical data of TA-IM ligands^a

Ligand	Emission λ_{max} (nm)	Excitation λ_{max} (nm)	Stokes shift (nm)	Φ_{PL} (%)	Intensity (a. u.)
5a	290	342	52	77	3837
5b	310	364	54	64	2318
5c	309	346	37	45	3154
5d	293	329	36	41	2062
5e	290	352	62	64	1836
5f	293	349	56	86	2935
5g	296	328	32	98	7246
5h	292	341	49	72	3576
5i	291	368	77	93	2780
5j	309	378	69	66	2532
5k	309	380	71	54	1717
6a	317	370	53	—	258
6b	—	—	—	—	47
6c	—	—	—	—	31

^a Fluorescence emission of compounds 5a–6c. Concentration: 20 $\mu\text{mol L}^{-1}$ in EtOH.

N-2-aryl triazole (NAT) system. Compared with NAT, TA-IM possessed similar UV-blue emission and comparable fluorescence intensity/efficiency, suggesting a similar planar intramolecular charge transfer (PICT) mechanism as proposed. With the fluorescence-active ligand available, we tested whether metal cation coordination may influence TA-IM fluorescence emission.

As shown in Fig. 3A, treating a solution of 5a with various metal cations (24 cations tested) showed almost no fluorescence change except for the Ag^+ cation. Notably, this highly selective Ag^+ induced fluorescence quenching is very efficient (92%) under mild conditions (room temperature). Impressively, this Ag^+ sensing was very robust, showing almost no influence of other cations and anions (no significant change while combining Ag^+ with more than 30 cations and anions, see details in Fig. S7 and S8†). This result is interesting and suggests that TA-IM can be developed as a potential fluorescent sensor toward Ag^+ detection. Since silver and silver ion-containing materials have been increasingly used in industry,¹² a large amount of non-biodegradable silver ions from industrial wastes is being discharged into the environment.¹³ This could cause severe harm to the environment¹⁴ and human health.¹⁵ Hence, establishment of an efficient and reliable sensor for the Ag^+ detection is in great demand.

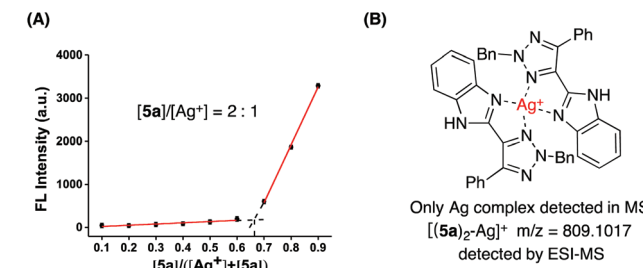


Fig. 4 (A) Job's plot: total concentration of 5a^a and Ag^+ was 10 $\mu\text{mol L}^{-1}$. (B) ESI-MS of the $[(5a)_2\text{-Ag}]^+$ ion. ^aEtOH : HEPES, v : v = 1 : 99.

As shown in Fig. 3A, the high selectivity of TA-IM for the detection of Ag^+ is due to the strong coordination between the ligand and Ag^+ . The fluorescence lifetime of 5a was monitored (Fig. S11†), showing no changes in the absence and presence of Ag^+ . This result suggested that the observed silver cation sensing was attributed to static quenching as proposed.¹⁶

One important feature of any cation fluorescent probe is the response time. As shown in Fig. 5A, the solution fluorescence intensity decreased immediately upon treating with silver cations and reached equilibrium within 20 seconds. To the best of our knowledge, this sensing response rate is faster than any previously reported Ag^+ fluorescent probes.¹⁷ Moreover, the FL emission intensity of 5a solution remained stable even after 120 min irradiation treatment with a xenon lamp (Fig. S12†). Detection within the pH range from 4.0 to 9.0 was performed with no clear drop of sensitivity and stability.

Based on the Benesi–Hildebrand equation, the binding association constant K_a was determined as $1.01 \times 10^7 \text{ M}^{-2}$, suggesting a strong coordination between the ligand and Ag^+ (Fig. S10†). The fluorescence lifetime of 5a was monitored (Fig. S11†), showing no changes in the absence and presence of Ag^+ . This result suggested that the observed silver cation sensing was attributed to static quenching as proposed.¹⁶

One important feature of any cation fluorescent probe is the response time. As shown in Fig. 5A, the solution fluorescence intensity decreased immediately upon treating with silver cations and reached equilibrium within 20 seconds. To the best of our knowledge, this sensing response rate is faster than any previously reported Ag^+ fluorescent probes.¹⁷ Moreover, the FL emission intensity of 5a solution remained stable even after 120 min irradiation treatment with a xenon lamp (Fig. S12†). Detection within the pH range from 4.0 to 9.0 was performed with no clear drop of sensitivity and stability.

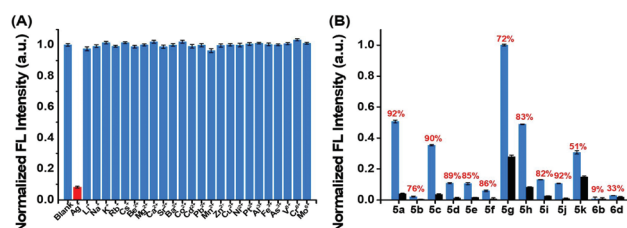


Fig. 3 (A) The high selectivity of TA-IM for the detection of Ag^+ . (B) Sensitivity of all TA-IM (5a–5k) in response to silver cations. Concentration: 5a–5k, 2 $\mu\text{mol L}^{-1}$; metal ions, 2 $\mu\text{mol L}^{-1}$; EtOH : HEPES, v : v = 1 : 99. The blue bar is the normalized FL intensity of 5a–6d; the blank bar is the FL intensity of 5a–6d after treating with Ag^+ ; the red number is the quenching ratio of FL.

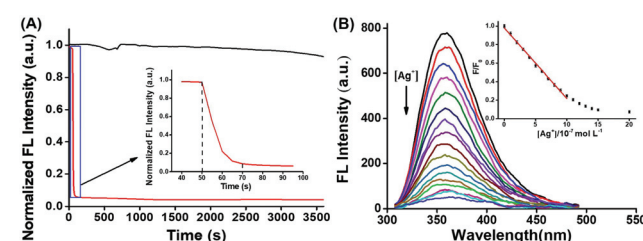


Fig. 5 (A) Time dependent titration of 5a (2 $\mu\text{mol L}^{-1}$) with Ag^+ (2 $\mu\text{mol L}^{-1}$); (B) linear correlation of $[\text{Ag}^+]$ and FL emission. EtOH : HEPES, v : v = 1 : 99.

lity (Fig. S13†). All these features (ultrafast response time, excellent stability and a wide pH operating range in aqueous medium) make TA-IM a promising fluorescent sensor for Ag^+ detection.

Finally, to establish the quantitative detection curve, titration of Ag^+ with the TA-IM ligand was performed (Fig. 5B). At a concentration from 1.0×10^{-7} to 1.0×10^{-6} mol L⁻¹, a good linear correlation between the fluorescence intensity and Ag^+ concentration was obtained with $R^2 = 0.9948$. The detection limit (LOD) was calculated to be 9.4 nmol L⁻¹ (based on S/N = 3, $n = 20$). To the best of our knowledge, this is much lower than the previously reported fluorescent probes (see the detailed comparison of TA-IM with the reported Ag^+ sensors in ESI, Table S5†).

Conclusions

In summary, we have successfully developed triazole-imidazole ligands as highly selective fluorescent probes for detection of silver ions. The introduction of an intramolecular H-bond allows TA-IM to exhibit strong emission in both organic and aqueous solutions. This sensor can be used in aqueous media with an ultrafast response time (<30 s), which highlights the practical advantages of this new cation probe and the importance of these triazole-based fluorescence compounds in chemical and material research.

Conflicts of interest

There are no conflicts to declare.

Acknowledgements

We are grateful to the NSF (CHE-1665122), the NIH (1R01GM120240-01), the NSFC (21629201) and the Development Project of the Pharmaceutical Industry of Jilin Province (20150311070YY; 20170307024YY) for financial support.

Notes and references

- 1 (a) Y. Hong, J. Lam and B. Tang, *Chem. Commun.*, 2009, 4332–4353; (b) J. H. Viles, *Coord. Chem. Rev.*, 2012, **256**, 2271–2284; (c) H. Zhu, J. Fan, B. Wang and X. Peng, *Chem. Soc. Rev.*, 2015, **44**, 4337–4366; (d) S. Jung and X. Chen, *Adv. Healthcare Mater.*, 2018, **7**, 1800252.
- 2 (a) Z. Guo, S. Park, J. Yoon and I. Shin, *Chem. Soc. Rev.*, 2014, **43**, 16–29; (b) D. Ding, K. Li, B. Liu and B. Tang, *Acc. Chem. Res.*, 2013, **46**, 2441–2453.
- 3 (a) X. Qian and Z. Xu, *Chem. Soc. Rev.*, 2015, **44**, 4487–4493; (b) H. Cheng, J. Yoon and H. Tian, *Coord. Chem. Rev.*, 2018, **372**, 66–84; (c) H. Kobayashi, M. Ogawa, R. Alford, P. L. Choyke and Y. Urano, *Chem. Rev.*, 2009, **110**, 2620–2640.

- 4 (a) J. Chan, S. Dodani and C. Chang, *Nat. Chem.*, 2012, **4**, 973–984; (b) M. Formica, V. Fusi, L. Giorgi and M. Micheloni, *Coord. Chem. Rev.*, 2012, **256**, 170–192; (c) L. M. Hyman and K. J. Franz, *Coord. Chem. Rev.*, 2012, **256**, 2333–2356; (d) M. Gao and B. Z. Tang, *ACS Sens.*, 2017, **2**, 1382–1399.
- 5 (a) G. Aromí, L. Barrios, O. Roubeau and P. Gamez, *Coord. Chem. Rev.*, 2011, **255**, 485–546; (b) D. Huang, P. Zhao and D. Astruc, *Coord. Chem. Rev.*, 2014, **272**, 145–165.
- 6 (a) W. Yan, X. Ye, N. G. Akhmedov, J. L. Petersen and X. Shi, *Org. Lett.*, 2012, **14**, 2358–2361; (b) R. Cai, W. Yan, M. G. Bologna, K. de Silva, Z. Ma, H. O. Finklea, J. L. Petersen, M. Li and X. Shi, *Org. Chem. Front.*, 2015, **2**, 141–144; (c) S. Hosseyni, S. Ding, Y. Su, N. Akhmedov and X. Shi, *Chem. Commun.*, 2016, **52**, 296–299; (d) R. Cai, X. Ye, Q. Sun, Q. He, Y. He, S. Ma and X. Shi, *ACS Catal.*, 2017, **7**, 1087–1092; (e) Y. Chen, W. Yan, N. Akhmedov and X. Shi, *Org. Lett.*, 2010, **12**, 344–347; (f) D. Wang, X. Ye and X. Shi, *Org. Lett.*, 2010, **12**, 2088–2091.
- 7 (a) Y. Chen, Y. Liu, J. L. Petersen and X. Shi, *Chem. Commun.*, 2008, 3254–3256; (b) S. Sengupta, H. Duan, W. Lu, J. L. Petersen and X. Shi, *Org. Lett.*, 2008, **10**, 1493–1496.
- 8 (a) Y. Liu, W. Yan, Y. Chen, J. L. Petersen and X. Shi, *Org. Lett.*, 2008, **10**, 5389–5392; (b) W. Yan, Q. Wang, Q. Lin, M. Li, J. L. Petersen and X. Shi, *Chem. – Eur. J.*, 2011, **17**, 5011–5018.
- 9 (a) H. Duan, S. Sengupta, J. L. Petersen and X. Shi, *Organometallics*, 2009, **28**, 2352–2355; (b) W. Liao, Y. Chen, Y. Liu, H. Duan, J. L. Petersen and X. Shi, *Chem. Commun.*, 2009, 6436–6438; (c) Y. Chen, D. Wang, J. L. Petersen, N. G. Akhmedov and X. Shi, *Chem. Commun.*, 2010, **46**, 6147–6149; (d) X. Ye, Z. He, T. Ahmed, K. Weise, N. G. Akhmedov, J. L. Petersen and X. Shi, *Chem. Sci.*, 2013, **4**, 3712–3716; (e) D. Ghosh, S. Rhodes, K. Hawkins, D. Winder, A. Atkinson, W. Ming, C. Padgett, J. Orvis, K. Aiken and S. Landge, *New J. Chem.*, 2015, **39**, 295–303; (f) P. A. Scattergood, A. Sinopoli and P. I. P. Elliott, *Coord. Chem. Rev.*, 2017, **350**, 136–154; (g) Q. J. Meisner, J. V. Accardo, G. Hu, R. J. Clark, D. E. Jiang and L. Zhu, *J. Phys. Chem. A*, 2018, **122**, 2956–2973.
- 10 (a) G. Aromí, L. A. Barrios, O. Roubeau and P. Gamez, *Coord. Chem. Rev.*, 2011, **255**, 485–546; (b) D. Huang, P. Zhao and D. Astruc, *Coord. Chem. Rev.*, 2014, **272**, 145–165.
- 11 For reviews on fluorescent sensors for metal detection: (a) P. Jiang and Z. Guo, *Coord. Chem. Rev.*, 2004, **248**, 205–229; (b) Z. Xu, X. Chen, H. N. Kim and J. Yoon, *Chem. Soc. Rev.*, 2010, **39**, 127–137; (c) G. Aragay, J. Pons and A. Merkoci, *Chem. Rev.*, 2011, **111**, 3433–3458; (d) Y. Jeong and J. Yoon, *Inorg. Chim. Acta*, 2012, **381**, 2–14; (e) H. N. Kim, W. X. Ren, J. S. Kim and J. Yoon, *Chem. Soc. Rev.*, 2012, **41**, 3210–3244; (f) J. Yin, Y. Hu and J. Yoon, *Chem. Soc. Rev.*, 2015, **44**, 4619–4644; (g) B. Kaur, N. Kaur and S. Kumar, *Coord. Chem. Rev.*, 2018, **358**, 13–69; (h) G. Sivaraman, M. Iniya, T. Anand, N. G. Kotla,

O. Sunnapu, S. Singaravel, A. Gulyani and D. Chellappa, *Coord. Chem. Rev.*, 2018, **357**, 50–104.

12 Y. Wen, F. Xing, S. He, S. Song, L. Wang, Y. Long, D. Li and C. Fan, *Chem. Commun.*, 2010, **46**, 2596–2598.

13 K. Mao, Z. Wu, Y. Chen, X. Zhou, A. Shen and J. Hu, *Talanta*, 2015, **132**, 658–663.

14 J. Zhang, Y. Zhou, J. Yoon and J. Kim, *Chem. Soc. Rev.*, 2011, **40**, 3416–3429.

15 (a) A. Lansdown, *Silver in Healthcare: Its Antimicrobial Efficacy and Safety in Use*, Royal Society of Chemistry, UK, 2010; (b) R. Tupling and H. Green, *J. Appl. Physiol.*, 2002, **92**, 1603–1610; (c) G. Gould, J. Colyer, J. East and A. Lee, *J. Biol. Chem.*, 1987, **262**, 7676–7679.

16 (a) I. Kim, N. E. Lee, Y. J. Jeong, Y. H. Chung, B. K. Cho and E. Lee, *Chem. Commun.*, 2014, **50**, 14006–14009; (b) Y. Fang, C. Li, L. Wu, B. Bai, X. Li, Y. Jia, W. Feng and L. Yuan, *Dalton Trans.*, 2015, **44**, 14584–14588.

17 Methods have been applied for Ag(i) determination, such as atomic absorption spectrometry, see: P. Liang and L. Peng, *Microchim. Acta*, 2010, **168**, 45–50. Inductively coupled plasma mass spectrometry: C. Gautier, M. Bourgeois, H. Isnard, A. Nonell, G. Stadelmann and F. Goutelard, *J. Chromatogr. A*, 2011, **31**, 5241–5247. Voltammetry: F. Wang, Q. Liu, Y. Wu and B. Ye, *J. Electroanal. Chem.*, 2009, **630**, 49–54. For fluorescent probes, see: (a) S. Singha, D. Kim, H. Seo, S. W. Cho and K. H. Ahn, *Chem. Soc. Rev.*, 2015, **44**, 4367–4399; (b) J. F. Zhang, Y. Zhou, J. Yoon and J. S. Kim, *Chem. Soc. Rev.*, 2011, **40**, 3416–3429; (c) L. Xu, Y. Xu, W. Zhu, C. Yang, L. Han and X. Qian, *Dalton Trans.*, 2012, **41**, 7212–7217; (d) L. Zhang, Y. Jian, J. Wang, C. He, X. Li, T. Liu and C. Duan, *Dalton Trans.*, 2012, **41**, 10153–10155; (e) J. Sun, Y. Yue, P. Wang, H. He and Y. Jin, *J. Mater. Chem. C*, 2013, **1**, 908–913; (f) Y. P. Zhou, E. B. Liu, J. Wang and H. Y. Chao, *Inorg. Chem.*, 2013, **52**, 8629–8637; (g) T. Anand, G. Sivaraman, P. Anandh, D. Chellappa and S. Govindarajan, *Tetrahedron Lett.*, 2014, **55**, 671–675; (h) L. Bian, X. Ji and W. Hu, *J. Agric. Food Chem.*, 2014, **62**, 4870–4877; (i) Y. Zhang, H. Jiang and X. Wang, *Anal. Chim. Acta*, 2015, **870**, 1–7; (j) A. N. Kursunlu and E. Güler, *J. Mol. Struct.*, 2017, **1134**, 345–349; (k) H. Wu, J. Jia, Y. Xu, X. Qian and W. Zhu, *Sens. Actuators, B*, 2018, **265**, 59–66; (l) P. K. Upadhyay, S. B. Marpu, E. N. Benton, C. L. Williams, A. Telang and M. A. Omary, *Anal. Chem.*, 2018, **90**, 4999–5006; (m) S. Singha, D. Kim, H. Seo, S. W. Cho and K. H. Ahn, *Chem. Soc. Rev.*, 2015, **44**, 4367–4399; (n) D. Shi, X. Wei, Y. Sheng, Y. Zang, X. He, J. Xie, G. Liu, Y. Tang, J. Li and G. Chen, *Sci. Rep.*, 2014, **4**, 4252–4258.